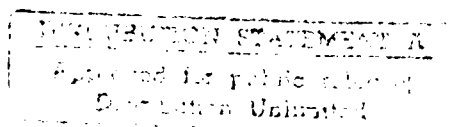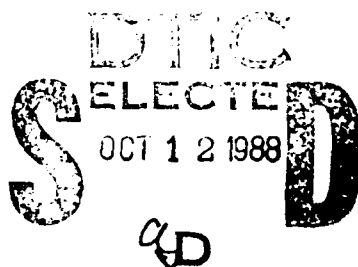AD-A200 446

UCLA School of Engineering and Applied Science

Department of Civil Engineering                               UCLA-ENG-88-07

## Micromechanics of An Extrusion

## in High Cycle Fatigue

T.H.Lin
S.R.Lin
X.Q.Wu

88 9

# Micromechanics of An Extrusion in
# High-Cycle Fatigue[*]

by

T.H. Lin[**], S.R. Lin[***], and X.Q. Wu[**]

## Abstract

A most favorably oriented crystal located at a free surface of a f.c.c. polycrystal under cyclic tension and compression of high-cycle loading is considered. An extrusion in this crystal is shown to be caused by a positive slip in one thin slice "P" and a negative slip in a closely located slice "Q". An initial tensile strain $e^i_{\alpha\alpha}$ in the thin slice "R" sandwiched between P and Q causes an initial compressive stress $\tau^i_{\alpha\alpha}$ in R and a positive initial shear stress $\tau^i_{\alpha\beta}$ in P and a negative one in Q. (The repetition of the subscript in Greek letters in this paper as the above does not denote summations). Slices P, Q and R, slip direction $\alpha$ and normal to the slip plane $\beta$ all make 45° with the free surface. The elongation in R induced by this initial strain is called the "static extrusion". The difference in resolved shear stresses in P and Q causes the build-up of plastic shear strain in P and Q, hence the extrusion growth. As the extrusion grows, the initial compression in R decreases resulting in a decrease in the extrusion growth rate. This decrease of compression in R tends to activate a second slip system to slide. The plastic strain due to slip in this second slip system has *a tensor component*

*1*

$e''_{\alpha\alpha}$, which has the same effect as the initial strain $e^i_{\alpha\alpha}$ in causing the positive and negative resolved shear stresses in P and Q, and hence the additional extrusion growth. In the present study with the consideration of the secondary slip in R, the extrusion is shown to grow far beyond the static extrusion. A similar conclusion can be made for the growth of an intrusion.

## Introduction

Forsyth (1953) made an important discovery of extrusion and intrusion in fatigue bands in aluminum alloys. Thompson, Wadsworth and Louat (1956) and Hall (1958) detected extrusions in both copper and aluminum. Extrusions were observed by Meke and Blochwitz (1980) and Mughrabi (1980) in their studies of persistent slip bands. Extrusions and intrusions in fatigue specimens were also observed by a number of other investigators.

Following the clue, provided by the observation on extrusions and intrusions, a number of theories of fatigue crack initiation have been proposed by different distinguished investigators: Mott (1958), Cottrell and Hull (1957), Thompson (1959), McEviley and Machlin (1959), Wood (1956) and others. One theory considered a column of metal containing a single screw dislocation intersecting a free surface. Assuming that this dislocation travels a complete circuit, the volume contained in the circuit is translated parallel to the dislocation. This causes the metal to extrude. However, this mechanism does not explain why the dislocation under cyclic stressing does not oscillate back and forth along the same path rather than transversing a closed circuit. Clearly, some form of gating mechanism is required to convert the back and forth oscillation of the dislocation into a uni-directional circuit. This gating mechanism is also needed in a number of other proposed mechanisms as discussed by Kennedy (1963).

It is well known that single crystal tests show that, under stress, slip occurs along certain directions on certain planes; this slip depends on the resolved shear stress and not on the normal stress on the sliding plane. This dependency of slip on the resolved shear stress, known as Schmid's law, has been shown by Parker (1961) to hold also under cyclic loadings. Hence to calculate the slip distribution in a fatigue band, we need to calculate the resolved shear stress distribution in the band.

Referring to a set of rectangular coordinates, we consider the strain to consist of the elastic part $e'_{ij}$ and the inelastic part $e''_{ij}$:

$$e_{ij} = e'_{ij} + e''_{ij}$$

(1)

The inelastic strain may be a combination of thermal strain, $e^T_{ij}$, creep strain $e^C_{ij}$, plastic strain $e^P_{ij}$ and initial strain $e^I_{ij}$. Consider the elastic constants to be isotropic. The stress is related to the elastic strain as

$$\tau_{ij} = \delta_{ij}\,\lambda e'_{kk} + 2G\,e'_{ij}$$

(2)

where $\lambda$ and $G$ are Lame's constants, $\delta_{ij}$ is the Kronecker delta and the repetition of subscript denotes summation.

The condition of static equilibrium is written as

$$\tau_{ij,j} + F_i = 0 \quad ; \quad \tau_{ij}v_j = T^v_i$$

(3)

where the subscript after comma denotes differentiation with respect to the coordinate variable; $F_i$, is the i-th component of the body force and $T^v_i$ is the i-th component of the surface traction on the surface with outward unit normal $v$.

3

Substituting Eq. (2) into Eq. (3) yields

$$\lambda e_{kk,i} + 2\,Ge_{ij,j} + F_i - (\lambda e''_{kk,i} + 2G\,e''_{ij,j}) = 0 \tag{4}$$

$$(\lambda e_{kk}\,\delta_{ij} + 2\,Ge_{ij})\,v_j = T_i^v + (\lambda e''_{kk}\,\delta_{ij} + 2\,Ge''_{ij})\,v_j \tag{5}$$

It is seen that $-(\lambda e''_{kk,i} + 2Ge''_{ij,j})$ is equivalent to $F_i$ and $(\lambda e''_{kk}\,\delta_{ij} + 2Ge''_{ij})v_j$ is equivalent to $T_i^v$ in causing the strain field $e_{ij}$; hence they are called equivalent body and surface forces and are denoted by $\overline{F}_i$ and $\overline{T}_i^v$ respectively. The stress field is then

$$\tau_{ij} = \delta_{ij}\,\lambda\,(e_{kk} - e''_{kk}) + 2G(e_{ij} - e''_{ij}) \tag{6}$$

Hence, the strain distribution in a body with inelastic strains under an external load is the same as that in a purely elastic body without inelastic strains but with additional equivalent body and surface forces. This analogy reduces to Duhammel's analogy of thermal stress (Lin, 1968) when the inelastic strain is thermal strain and gives the same results as those given by Eshelby's ingenious process of cutting, relaxing, restoring, welding, and relieving in his famous paper on ellipsoidal inclusions (Eshelby, 1959). This method of equivalent force is here used to calculate the stress fields in fatigue bands.

**A Polycrystal Model**

Fatigue cracks generally initiate at a free surface. To relieve the same amount of resolved shear stress in a thin slice, a greater amount of slip i.e., plastic strain, is required near the free surface than at the interior of metals (Lin and Ito, 1967). For the present analytical study, the thin slices subjected to alternate forward and reversed loadings are taken to be in the most favorably-oriented crystal at the free surface of a polycrystal. The slip plane and

4

the slip direction of the most favorable slip system of this crystal form 45° with the specimen axis. The polycrystal is subject to a cyclic tension and compression of low amplitude, so the plastic deformation essentially occurs only in this most favorably oriented crystal.

Defects exist in all metals. The initial resolved shear stress field caused by initial defects is denoted by $\tau^i$. During loading, when the critical shear stress is exceeded in some region, slip occurs. After unloading, this slip remains and induces a residual resolved shear stress field $\tau^r$. The resolved shear stress caused by loading is denoted by $\tau^a$. Hence, the total resolved shear stress is the sum of these three stresses: $\tau^i + \tau^r + \tau^a$.

For an extrusion to initiate, positive shear has to occur in a thin slice P and negative shear in a closely located slice Q, as shown in Figure 1. The initial stress field $\tau^i$ favorable for this slip sequence is one having positive shear stress in P and negative in Q. Lin and Lin (1983) have shown that such an initial stress field can be provided by an initial strain in the thin slice R, sandwiched between P and Q. Referring to Fig. 1, an initial strain field $e^i_{\alpha\alpha}$ varying linearly from zero at the free surface to a maximum value at the interior boundary of the crystal, causes a constant gradient of strain $e^i_{\alpha\alpha}$ along the $\alpha$ direction and a uniform equivalent body force $\overline{F}_\alpha$ in R yielding a uniform initial positive resolved shear stress $\tau^i$ in P and a negative one in Q. Lin and Ito (1969) suggested that this positive $e^i_{\alpha\alpha}$ can be produced by a row of interstitial dislocation dipoles, and a negative $e^i_{\alpha\alpha}$ by vacancy dipoles. Recently, Antoncpoulus, Brown and Winter (1976) and Mughrabi, Wang, Differt and Essmann (1983) have shown that the ladder structure in a persistent slip band (PSB) can be represented by an array of dislocation dipoles causing initial resolved shear stresses at the interface between the PSB and the matrix.
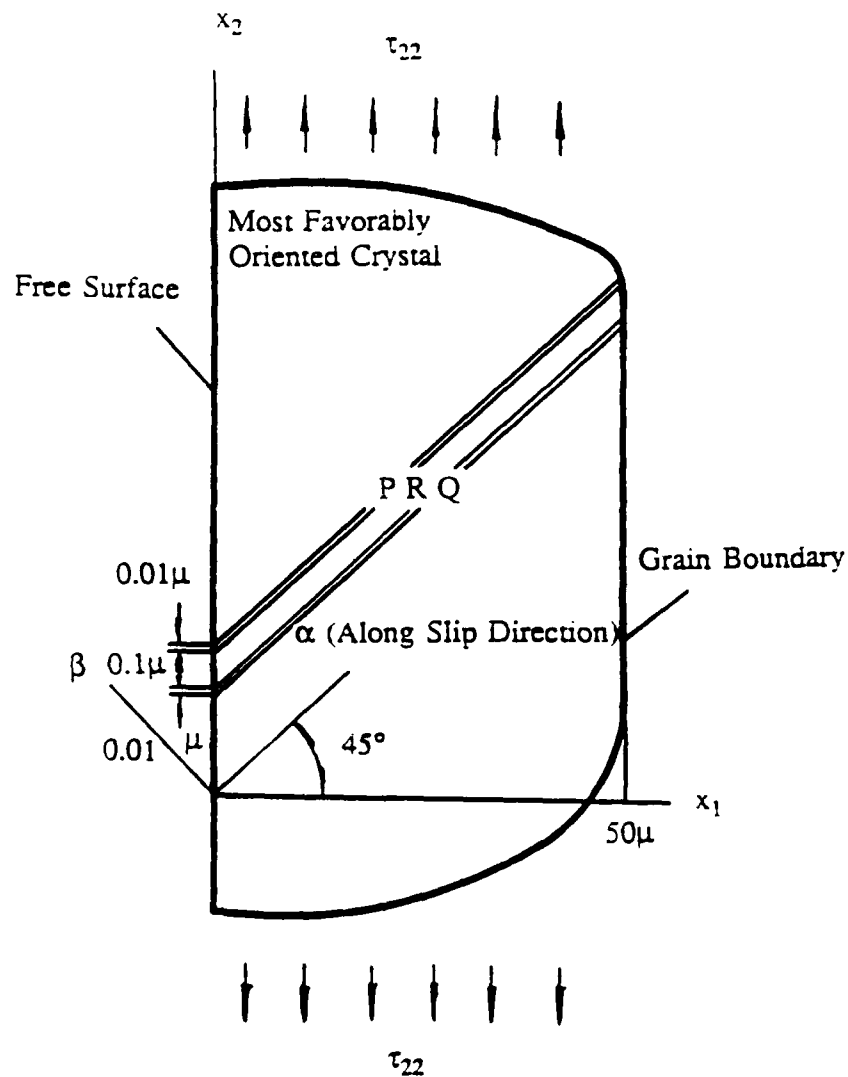
Fig.1 Most Favorably Oriented

Crystal at Free Surface

## Gating Mechanism Provided by Micro Stress Fields:

Consider $\tau^i$ to be positive in P and negative in Q as that caused by an array of interstitial dislocation dipoles discussed earlier. Referring to Fig. 1, a tensile loading causes a positive resolved shear stress $\tau_a$ in this crystal. In P the shear stress will be the sum of $\tau_i$ and $\tau_a$ and will be the first to reach the critical stress $\tau_c$ and slide first. The plastic strain and the equivalent forces are taken to be constant along the $x_3$ direction, $\partial\tau_{\alpha3}/\partial x_3 = 0$. From the equilibrium condition Eq. (3), with no body force we have $\partial\tau_{\alpha\alpha}/\partial\alpha + \partial\tau_{\alpha\beta}/\partial\beta = 0$, where $\beta$ is normal to the slip plane. Since $\partial\tau_{\alpha\alpha}/\partial\alpha$ is finite, $\partial\tau_{\alpha\beta}/\partial\beta$ is also finite and the change of $\tau_{\alpha\beta}$ across the short distance between P and Q is very small. Therefore, the slip in P relieves not only the positive shear stress in P, but also in its neighboring region including Q as shown by Lin and Ito (1969) and Lin (1977). This keeps the positive shear stress in the neighboring region from reaching that of P, hence only P slides during the forward loading. This slip increases the negative resolved shear stress in Q to cause Q to slide more readily in the reverse loading. When the negative resolved shear stress in Q reaches $\tau^c$ in the reversed loading, slip occurs in Q and a new residual stress field is produced. Similarly, the slip in Q causes the relief of negative resolved shear stress not only in Q but also in its neighboring region including P, thus making P more readily to slide in the next forward loading. This process is repeated for every cycle, providing a natural gating mechanism for the monotonic buildup of local slip and plastic strain in P and Q. The plastic shear strains $e_{\alpha\beta}''$ in P and Q tend to push out the slice R and start an extrusion. Interchanging the signs of initial stresses in P and Q will initiate an intrusion instead of an extrusion. This theory is extensively supported by metallurgical observations (Lin, 1977). Some of them are given below.

## Some Related Experimental Observations

Slip lines are often developed in the early stage of fatigue cycling to produce "soft" regions where local deformation tends to concentrate as shown by Woods (1973), Winter (1974), Finney and Laird (1975). Slip lines generally multiply and grow into persistent slip bands. Persistent slip bands carry essentially all the plastic strain in low amplitude fatigue tests as indicated by Brown and Ogin (1984). Tests on aluminum single crystals under cyclic tension and compression by Charsley and Thompson (1963) have shown that a reversal of stress after a prior tensile deformation gives rise to new slip lines. Similar "compressive" slip lines were observed by Buckley and Entwistle (1956) to form between "tensile" slip lines. Forsyth (1954) found that the slip lines produced in the forward loading and those produced in the reversed loading were in the same fatigue band, very close but distinct from each other. Wood and Bendler (1962) have shown with their electron-micrographs, that both forward and backward slips have occurred within a fatigue band; also the slip that occurs in cyclic loading does not lead to significant deformation in the bulk of the matrix. This is verified by the lack of dark spots on the X-ray reflection photographs of fatigue specimens shown by Woods (1956). Intrusions are often considered as embryos of cracks. Other experimental observations and suggested models of fatigue crack initiation were given in two excellent reviews by Grosskreutz (1971) and Laird and Duquette (1972). These experimental observations show that the slip lines formed in the forward loading and those formed in the reversed loading in fatigue specimens often are closely spaced but distinct from each other. Observations clearly support the proposed gating mechanism provided by the microstress fields due to two alternatively sliding slices.

8

**Extent of Extrusion and Intrusion:**

The buildup of the slip strain $e_{\alpha 3}''$ in P and Q is caused by $e_{\alpha\alpha}^i$ in R. If R were cut out, the free length of R would be longer than the slot by an amount referred to as the "static extrusion" by Mughrabi et al. (1983). This $e_{\alpha\alpha}^i$ causes an initial compression $\tau_{\alpha\alpha}^i$ in R. Under cyclic loading, the extrusion grows and the thin slice R increases in length. This elongation causes the compression to decrease. A question raised by Mughrabi (1980) and Essmann, Gosele and Mughrabi (1981) is whether the extrusion growth will cease after the extrusion has reached the magnitude of the static extrusion. This question is to be discussed in the following calculations.

There are twelve slip systems in a f.c.c. crystal. The change of the direct stress $\tau_{\alpha\alpha}$ in R causes changes of resolved shear stresses in all slip systems. When the decrease of compression R becomes large, its resulting residual stresses combined with the applied stress can cause a second slip system to have shear stress reaching the critical and slide. The plastic strain $e_{\xi\eta}''$, caused by slip in this slip system has a tensor component $e_{\alpha\alpha}''$ just like $e_{\alpha\alpha}^i$ in causing the positive and negative $\tau_{\alpha\beta}^i$ in P and Q respectively. Hence this secondary slip can increase greatly the extent of extrusion and intrusion.

**Method for Calculating Incremental Slip in P, Q and R:**

The slip direction $\alpha$ and the normal to the slip plane $\beta$ make $45°$ to the loading axis (Fig. 1). As the extrusion grows, $e_{\alpha\sim}$ in the slip band causes $\tau_{\alpha\alpha}$ to increase and can cause a second slip system to slide. $\alpha\beta$ lie in the $x_1$, $x_2$ plane as shown in Fig. 1 but $\xi\eta$ is not confined to the $x_1$, $x_2$-plane. Hence the equivalent force $\underline{F_i}$ due to $e_{\xi\eta}''$ can have component

9

normal to this plane. In 1972, Lin and Lin showed the effect of a secondary slip on fatigue crack initiation. To simplify the numerical computation, they assumed the second slip system to be on the $x_1$-plane along the $x_2$ direction or vice-versa. This is not an actual slip system. In the present study, the second slip system analyzed is one actually existing in the crystal. The presence of a body force component along the $x_3$ direction requires the modification of the solution of the plane strain problem. A similar problem was shown in the analysis of prismatic anisotropic bars by Lekhnitski (1963) and is referred to as the generalized plane strain problem. This generalized plane strain is expressed as

$$u_i = u_i(x_1\ x_2), \quad i = 1,2,3$$

(7)

This gives

$$\tau_{ij} = 2G\left[\frac{v}{1-2v}\ \delta_{ij}\ \theta + \tfrac{1}{2}\ (u_{i,j} + u_{j,i})\right]$$

(8)

where $\theta = u_{1,1} + u_{2,2}$ and $v$ is Poisson's ratio. The substitution of this expression into the condition of equilibrium (3) yields

$$\nabla^2 u_\alpha + \frac{1}{1-2v}\ \frac{\partial\theta}{\partial x_\alpha} + \frac{F_\alpha}{G} = 0\ , \quad \alpha = 1,2$$

(9)

and

$$\nabla^2 u_3 + \frac{F_3}{G} = 0$$

(10)

The differential equations (9) and (10) are not coupled and can be solved separately.

The three slip directions of each of the four slip planes of a f.c.c. crystal are shown in Fig. 2. The most favorably oriented crystal of a polycrystal loaded under alternate tension and compression along the $x_2$ axis (Fig. 1) has a slip plane and a slip direction making 45° with the direction of loading. The slip system is referred to as the primary slip system. Let $a_2$ axis (Fig. 2), correspond to this system. During fatigue loading, the build-up of large local plastic shear strain in the primary slip system, positive in P and negative in Q, tends to start an extrusion or an intrusion. Consequently an appreciable direct stress $\tau_{\alpha\alpha}$ will be built-up in R. The Schmid's factors of all the 12 slip systems for the stress $\tau_{ij}$ and those for $\tau_{\alpha\alpha}$ are listed in Table 1. It is seen that there are four slip systems $c_1$, $c_3$, $d_1$ and $d_2$ equally favorable under $\tau_{\alpha\alpha}$. Among these four, $c_3$ is most favorably oriented under $\tau_{22}$ where $\tau_{22}$ is the alternate loading. Hence $c_3$ is considered to be the active second slip system in R.

Plastic strain $e''_{\alpha\beta}$ due to slip in the primary slip system $\alpha\beta$, causes equivalent forces $\underline{F}_1$ and $\underline{F}_2$. This is a plane strain problem Melan has given the solution of the stress distribution caused by a point force in a semi-infinite plate in plane stress. Melan's solution was modified for plane strain by Tung and Lin (1966). Let $\tau_{ij}^k$ (x, x̄) be the stress at x due to a unit force along $x_k$ axis applied at x̄ and $\phi_k$ (x, x̄) be the corresponding stress function, where x denotes $(x_1, x_2, x_3)$. Lin and Lin, 1974 has expressed the stress components in terms of the stress functions as:

$$\tau_{11}^k \ (x, \bar{x}) = \frac{\partial^2 \phi_k}{\partial x_2^2} \ , \quad \tau_{22}^k \ (x, \bar{x}) = \frac{\partial^2 \phi_k}{\partial x_1^2} \ , \quad \tau_{12}^k \ (x, \bar{x}) = - \frac{\partial^2 \phi_k}{\partial x_1 \partial x_2}, \quad k = 1,2 \tag{11}$$

where the stress functions are

11
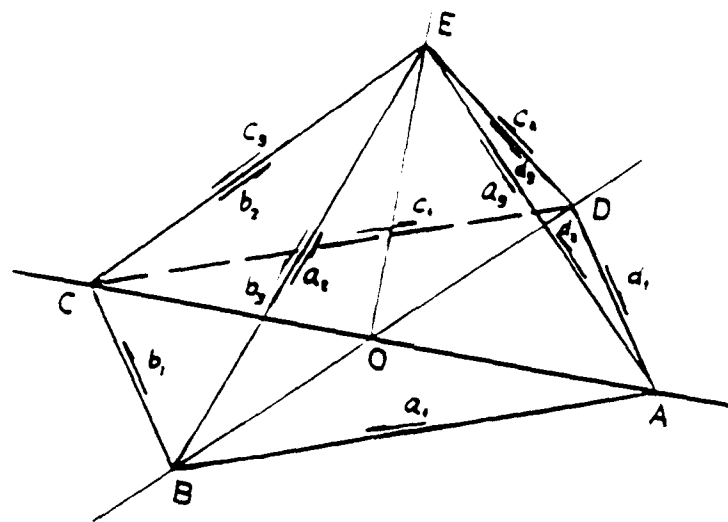
| Slip Planes | | Slip Directions | |
|---|---|---|---|
| Face | Plane | | |
| | | $a_1 = \frac{a}{2} [ 1\,\overline{1}\,0 ]$ | $c_1 = \frac{a}{2} [ \overline{1}\,1\,0 ]$ |
| "a" | ABE (1 1 1) | $a_2 = \frac{a}{2} [ \overline{1}\,0\,1 ]$ | $c_2 = \frac{a}{2} [ 1\,0\,1 ]$ |
| "b" | BCE (1 $\overline{1}$ 1) | $a_3 = \frac{a}{2} [ 0\,1\,\overline{1} ]$ | $c_3 = \frac{d}{1} [ 0\,\overline{1}\,\overline{1} ]$ |
| "c" | CDE ($\overline{1}\,\overline{1}$ 1) | $b_1 = \frac{a}{2} [ \overline{1}\,\overline{1}\,0 ]$ | $d_1 = \frac{a}{2} [ 1\,1\,0 ]$ |
| "d" | DAE ($\overline{1}$ 1 1) | $b_2 = \frac{a}{2} [ 0\,1\,1 ]$ | $d_2 = \frac{a}{2} [ 0\,\overline{1}\,1 ]$ |
| | | $b_3 = \frac{a}{2} [ 1\,0\,\overline{1} ]$ | $d_3 = \frac{a}{2} [ \overline{1}\,0\,\overline{1} ]$ |

Figure 2. Crystallographic Directions of a f.c.c. Crystal

12

Table 1. Resolved Shear Stresses in Different Slip System Caused by Cyclic Loading $\tau_{22}$ and $\tau_{uu}$ ($\alpha$ denotes $a_2$ Direction)

| SLIP SYSTEM | NORMAL TO SLIP PLANE $\xi(m)$ | SLIP DIRECTION $\eta(m)$ | DIRECTIONAL SCHMID FACTOR | | | | | | SCHMID FACTOR |
|---|---|---|---|---|---|---|---|---|---|
| | | | $\tau_{\xi\eta}/\tau_{11}$ | $\tau_{\xi\eta}/\tau_{12}$ | $\tau_{\xi\eta}/\tau_{13}$ | $\tau_{\xi\eta}/\tau_{22}$ | $\tau_{\xi\eta}/\tau_{23}$ | $\tau_{\xi\eta}/\tau_{33}$ | $\tau_{\xi\eta}/\tau_{uu}$ |
| $a_1$ | $(\frac{\sqrt{2}}{2}, \frac{\sqrt{2}}{2}, 0)$ | $(\frac{\sqrt{2}}{4}, \frac{\sqrt{2}}{4}, \frac{\sqrt{3}}{2})$ | 0.250 | 0 | 0.612 | 0.250 | -0612 | 0 | 0 |
| $a_2$ | | $(\frac{\sqrt{2}}{2}, \frac{\sqrt{2}}{2}, 0)$ | -0.500 | 0 | 0 | 0.500 | 0 | 0 | 0 |
| $a_3$ | | $(-\frac{\sqrt{2}}{4}, \frac{\sqrt{2}}{4}, \frac{\sqrt{3}}{2})$ | 0.250 | 0 | -0.612 | -0.250 | 0.612 | 0 | 0 |
| $b_1$ | $(\frac{\sqrt{2}}{6}, \frac{\sqrt{2}}{6}, \frac{2\sqrt{2}}{3})$ | $(\frac{\sqrt{2}}{4}+\frac{\sqrt{3}}{3}, \frac{\sqrt{2}}{4}, \frac{\sqrt{3}}{6})$ | -0.219 | 0.272 | -0.810 | -0.053 | 0.143 | 0.272 | 0 |
| $b_2$ | | $(\frac{\sqrt{2}}{4}, \frac{\sqrt{2}}{4}+\frac{\sqrt{3}}{3}, \frac{\sqrt{3}}{6})$ | 0.053 | -0.272 | 0.143 | +0.219 | -0.810 | -0.272 | 0 |
| $b_3$ | | $(\frac{\sqrt{2}}{2}, 0)$ | 0.164 | 0 | 0.667 | -0.164 | 0.667 | 0 | 0 |
| $c_1$ | $(-\frac{\sqrt{3}}{3}, -\frac{\sqrt{3}}{3}, \frac{\sqrt{2}}{6})$ | $(\frac{\sqrt{2}}{4}, \frac{\sqrt{3}}{3}, \frac{\sqrt{3}}{3})$ | 0.288 | 0.408 | 0.537 | 0.121 | 0.129 | -0.408 | 0.408 |
| $c_2$ | | $(\frac{\sqrt{2}}{4}+\frac{\sqrt{3}}{3}, \frac{\sqrt{2}}{4}, \frac{\sqrt{3}}{3})$ | -0.469 | 0.272 | -0.197 | 0.197 | -0.469 | 0.272 | 0 |
| $c_3$ | | $(\frac{\sqrt{2}}{4}, \frac{\sqrt{2}}{4}, \frac{\sqrt{3}}{6})$ | 0.182 | -0.680 | -0.340 | -0.318 | 0.340 | 0.136 | -0.408 |
| $d_1$ | $(-\frac{\sqrt{3}}{3}, \frac{\sqrt{2}}{6}, \frac{\sqrt{2}}{6})$ | $(\frac{\sqrt{2}}{4}, \frac{\sqrt{2}}{4}, \frac{\sqrt{3}}{2})$ | -0.318 | -0.680 | -0.340 | 0.182 | 0.340 | 0.136 | -0.408 |
| $d_2$ | | $(-\frac{\sqrt{3}}{3}, \frac{\sqrt{3}}{3}, \frac{\sqrt{3}}{6})$ | 0.121 | 0.408 | -0.129 | 0.288 | -0.537 | -0.408 | 0.408 |
| $d_3$ | | | -0.197 | -0.272 | -0.469 | 0.469 | -0.197 | -0.272 | 0 |

$$\phi_1(x, \overline{x}) = -(p+q)(x_2 - \overline{x}_2)(\theta_1 + \theta_2) + \tfrac{1}{2} q(x_1 - \overline{x}_1) \, l_n \, (X_1/X_2) + 2p \, \frac{x_1 \overline{x}_1(x_1 + x_1 + \overline{x}_1)}{X_2}$$

$$\phi_2(x, \overline{x}) = (p+q)(x_2 - \overline{x}_2)(\theta_1 + \theta_2) + \tfrac{1}{2} q(x_2 - \overline{x}_2) \, l_n \, (X_1/X_2) - 2p \, \frac{x_1 \overline{x}_1(x_2 + x_2 + \overline{x}_2)}{X_2}$$

$$\tag{12}$$

with

$$p = \frac{1}{4\pi(1-\nu)} \,, \quad q = p\,(1 - 2\nu),$$

$$\theta_1 = \arctan \left[ \frac{x_2 - \overline{x}_2}{x_1 \, \overline{x}_1} \right] \,, \quad -\pi \le \theta_1 < \pi$$

$$\theta_2 = \arctan \left[ \frac{x_2 - \overline{x}_2}{x_1 + \overline{x}_1} \right] \,, \quad -\frac{\pi}{2} \le \theta_2 < \frac{\pi}{2} \,,$$

$$X_1 = (x_1 - \overline{x}_1)^2 + (x_2 - \overline{x}_2)^2, \quad X_2 = (x_1 + \overline{x}_1)^2 + (x_2 - \overline{x}_2)^2$$

$$\tag{13}$$

Plastic strain $e_{\xi\eta}''$ due to slip in the secondary slip system causes $\underline{F}_3$ in addition to $\underline{F}_1$ and $\underline{F}_2$ To solve Eq. (10) for $\underline{F}_3$, we write $\phi_3 (x, \overline{x})$ as $G\, u_3(x, \overline{x})$. The stress is then

$$\tau_{13}^3 (x, \overline{x}) = \frac{\partial \phi_3}{\partial x_1} \;\; ; \;\; \tau_{23}^3 (x, \overline{x}) = \frac{\partial \phi_3}{\partial x_2}$$

$$\tag{14}$$

All other stress component's are zero. For a unit concentrated force $F_3$ at $\overline{x}$ Eq. 10 gives

$$\nabla^2 \, \phi_3 + \delta \, (x - \overline{x}) = 0$$

where $\delta(x, \overline{x})$ is the Dirac Delta function. With the boundary conditions of

14

$$\frac{\partial \phi_3}{\partial x_1} = 0 \text{ at } x_1 = 0 \text{ and}$$

$$\frac{\partial \phi_3}{\partial x_1} \text{ and } \frac{\partial \phi_3}{\partial x_2} \rightarrow 0 \text{ as } \sqrt{x_1^2 + x_2^2} \rightarrow \infty ,$$

(15)

we have

$$\phi_3(\mathbf{x}, \overline{\mathbf{x}}) = -\frac{1}{4} \pi \ (ln \ X_1 + ln \ X_2)$$

(16)

where $X_1$ and $X_2$ are given in Eq. 13.

**Numerical Calculation and Results:**

The thicknesses of the slices P, Q and R are very small as compared to their lengths. As discussed before, the slip strains in these slices are taken to be constant across the thickness. The slices are divided into a number of parallegram grids along the length in the $\alpha$ direction. For numerical calculation, a grid of constant plastic strain has been used. The corresponding grid stress is the average stress in the grid. From the plane strain solution of a semi-infinite medium the stress field caused by a uniform plastic strain $e_{\alpha\beta n}^{''}$ in the n-th grid was calculated. The relief of shear stress $\tau_{\alpha\beta}^{r}$ (x) at any point is expressed as

$$\tau_{\alpha\beta}^{r} (x) = - C (x, \alpha\beta \ ; \ n, \alpha\beta) \ e_{\alpha\beta_n}^{''}$$

(17)

where $C(x, \alpha\beta \ ; \ n, \alpha\beta)$ is the resolved shear stress at x due to unit uniform plastic strain $e_{\alpha\beta}^{''}$ in grid "n". The average relieved stress $\tau_{\alpha\beta}^{r}(x)$ over the m-th grid denoted by $\tau_{\alpha\beta_m}^{r}$ and is written as

15

$$\tau^r_{\alpha\beta_m} = - C (m, \alpha\beta ; \; n, \alpha\beta) \, e''_{\alpha\beta_n}$$

As a cyclic loading proceeds, slips occur in P and Q and cause a residual stress field. The total resolved shear stress in the $m^{th}$ grid of the $\alpha\beta$ slip system is the sum of the initial, residual and applied stresses:

$$\tau_{\alpha\beta_m} = \tau^i_{\alpha\beta_m} + \tau^a_{\alpha\beta_m} - \sum_n C (m, \alpha\beta ; \; n, \alpha\beta) \, e^n_{\alpha\beta_n} \qquad (18)$$

where "n" is summed over all the sliding grids with plastic strain $e''_{\alpha\beta_n}$.

Plastic deformation in metals is highly localized (Brown, 1952). Plastic strain concentrates in thin slices. The microscopic plastic strain in the thin slice is much larger than the macroscopic plastic strain in the metal. Hence, the strain-hardening of the thin slice is much less than that of the metal and is neglected. This gives a constant critical resolved shear stress $\tau^c$. Sliding occurs in the grids where $\tau(x) = \pm \tau^c$. For an incremental applied shear stress $\Delta \tau^a_m$, $\qquad \Delta \tau_m = \Delta \tau = 0$. Eq. 18 yields

$$\Delta \tau^a_{\alpha\beta_m} = \sum_n C (m, \alpha\beta ; \; n, \alpha\beta) \, \Delta e''_{\alpha\beta_n} \qquad (19)$$

There are as many unknown $\Delta e''_{\alpha\beta_n}$'s as the number of the above equations. The plastic strain increments $\Delta e''_{\alpha\beta_n}$ in the sliding grids for an incremental loading $\Delta \tau_a$ can be readily calculated. Similarly, the stress components $\tau^r_{\alpha\alpha}$ and $\tau^r_{\beta\beta}$ in R can be calculated (Lin, 1972) and written as

$$\tau^r_{\alpha\alpha_m} = \sum_n C (m, \alpha\alpha ; \; n, \alpha\beta) \, e''_{\alpha\beta_n} \qquad (20)$$

$$\tau^r_{\beta\beta_m} = \sum_n C(m, \beta\beta \; ; \; n, \alpha\beta) \, e''_{\alpha\beta_n}$$

From these calculations, it was found that $\tau^r_{\beta\beta_m}$ in R is quite small.

To find C $(m, \alpha\alpha \; ; \; n, \alpha\beta)$, a different approach, which gives a better physical insight, is considered. The elastic shear strain $e'_{\alpha\beta}$, that equals $\tau^c/2G$ in the sliding grids, is much less than the cumulative plastic strain $e''_{\alpha\beta}$. The cumulative plastic shear strain $e''_{\alpha\beta}$ in P and Q are about the same. Denoting the thickness of the slices P and Q by t, we can express the displacement in R along the $\alpha$ direction as $-2te_{\alpha\beta_{P,Q}}$ or approximately $-2te''_{\alpha\beta_{P,Q}}$. The negative sign is due to the fact that the direction of the extrusion is opposite to the direction of the $\alpha$ direction. This causes a tensile strain in R,

$$e''_{\alpha\alpha_R} = -2t \frac{\partial e_{\alpha\beta_{P,Q}}}{\partial \alpha} \tag{21}$$

Since $\tau^r_{\beta\beta}$ is very small and assumed to be zero, we have the residual tensile stress

$$\tau^r_{\alpha\alpha} = \frac{E}{1-v^2} \frac{\partial e''_{\alpha\beta}}{\partial \alpha} \tag{22}$$

With the residual stress $\tau^r_{\alpha\alpha}$ increasing with cycles of loading, the initial compressive stress $\tau^i_{\alpha\alpha}$ is gradually relieved.

As discussed earlier, $c_3$ (Table I) is the most likely second slip system to become active. The resolved shear stress in $c_3$ is denoted by $\tau_{\xi\eta}$. As shown in Table 1, the initial resolved shear stress $\tau^i_{\xi\eta}$ varies with the initial stress components $\tau^i_{13}, \tau^i_{23}, \tau^i_{33}$. For our numerical calculation $\tau^i_{\xi\eta}$ is assumed to be zero. From Table 1,

17

$$\Delta \tau_{\xi\eta} = -.318 \Lambda \tau_{22} - 0.408 \Delta \tau_{\alpha\alpha}$$

$$(23)$$

When $\tau_{\xi\eta}$ increase to $\tau^c$ or decreases to $-\tau^c$, this slip system slides and causes $e''_{\xi\eta}$. Now we have slip in the $\alpha\beta$ slip system in P and Q and in the $\xi\eta$ slip system in R.

Let the two slices P and Q be divided into 2N grids and R into M grids. The resolved shear stress in the $\alpha\beta$ slip system of the i-th grid is written as

$$\tau^r_{\alpha\beta_i} = -C(i, \alpha\beta \; ; \; j, \alpha\beta) \, e''_{\alpha\beta_j} - C(i, \alpha\beta \; ; \; k, \xi\eta) \, e''_{\xi\eta_k}$$

$$(24)$$

$$\tau^r_{\xi\eta_i} = -C(i, \xi\eta \; ; \; j, \alpha\beta) \, e''_{\alpha\beta_j} - C(i, \xi\eta \; ; \; k, \xi\eta) \, e''_{\xi\eta_k}$$

The repetition of subscript "j" denotes summation from one to 2N and that of subscript "k" denotes summation from one to M. $C(i, \xi\eta \; ; \; j, \alpha\beta)$ is the residual stress $\tau^r_{\xi\eta}$ in i-th grid due to a unit plastic strain $e''_{\alpha\beta}$ in the j-th grid. For constant strain $e''_{\alpha\beta}$ in grid, j the corresponding $C(i, \xi\eta \; ; \; j, \alpha\beta)$ is the average shear stress $\tau_{\xi\eta}$ in the i-th grid. A method of numerical calculation using grids with strain linear in $\alpha$ direction has also been developed and used. With residual stresses given by Eq. (24), the incremental plastic strain in all grids are calculated by Eq. (19).

The dimensions of the most favorably-oriented crystal at the free surface are shown in Fig. 1. The thickness in P and Q is 0.01 $\mu$ along $x_2$ dimension and thickness in R is 0.1 $\mu$ along the same direction. The initial strain $e^i_{\alpha\alpha}$ in R is assumed to vary linearly from zero at the free surface to $3.64 \times 10^{-5}$ at $x_1 = 50\mu$. The static extrusion is then $\frac{1}{2}$ x. $3.64 \times 10^{-5}$ x $50 \times \sqrt{2} \, \mu = 1.28 \times 10^{-3} \, \mu$. $e''_{\alpha\beta} = \frac{1}{2} \frac{\partial u_\alpha}{\partial \beta}$. This corresponds to a plastic strain $e''_{\alpha\beta}$ in P and Q at the free surface of 0.091.

18

This initial strain field causes a uniform initial shear stress of 1.46 x $10^{-3}$ MPa (0.20 p.s.i.) in P and -1.46 x $10^{-3}$ MPa (0.20 p.s.i.) in Q. The polycrystal is subject to a cyclic tensile and compressive loading in the $x_2$ direction. Let $\tau^E$ be the excessive shear stress defined as the initial shear stress $\tau^i$ plus the maximum applied shear stress $\tau^a$ minus the critical shear stress $\tau^c$:

$$\tau^E = \tau^i + \tau^a - \tau^c$$

(25)

Tests on single aluminum crystals under cyclic loading under constant plastic strain amplitude by Snowden, 1963, show that the resolved shear stress increases in the first 50 cycles and approaches a saturated value of about 2.94 MPa (425.8 p.s.i. or $300gm/nm^2$). Hence $\tau^c$ is taken as 2.94 MPa (425.8 p.s.i.). For a maximum applied shear stress $\tau^a$ of 2.94 MPa (425.8 p.s.i.), the excessive shear stress $\tau^E$ is 1.46 x $10^{-3}$ MPa (0.20 p.s.i.).

With the process of sliding discussed earlier, the plastic strain distributions $e_{\xi\eta}''$ in the secondary slip system are shown in Fig. 3 and the corresponding resolved shear stress ($\tau_{\xi\eta}$) variations are shown in Fig. 4. *The plastic strain $e_{\xi\eta}''$ in the second slip system causes some $e_{\alpha\alpha}''$, which in turn, causes positive $\tau_{\alpha\beta}$ in P and a negative $\tau_{\alpha\beta}$ in Q just like the initial strain $e_{\alpha\alpha}^i$.* This $e_{\xi\eta}''$ causes additional $+\tau_{\alpha\beta}$ in P and $-\tau_{\alpha\beta}$ in Q. The sum of the initial plus residual shear stresses $\tau_{\alpha\beta}^i + \tau_{\alpha\beta}^r$, in P and Q, on which the extrusion growth depends, is shown in Fig. 5. It is seen that this sum is considerably more in the cases with the secondary slip than in those without. The plastic shear strain distributions $e_{\alpha\beta}''$ in P and Q at different cycles of loading were calculated for the cases with and without the secondary slip and are shown respectively as solid and dotted lines in Fig. 6. The $e_{\alpha\beta}''$'s at the free surfaces vs.
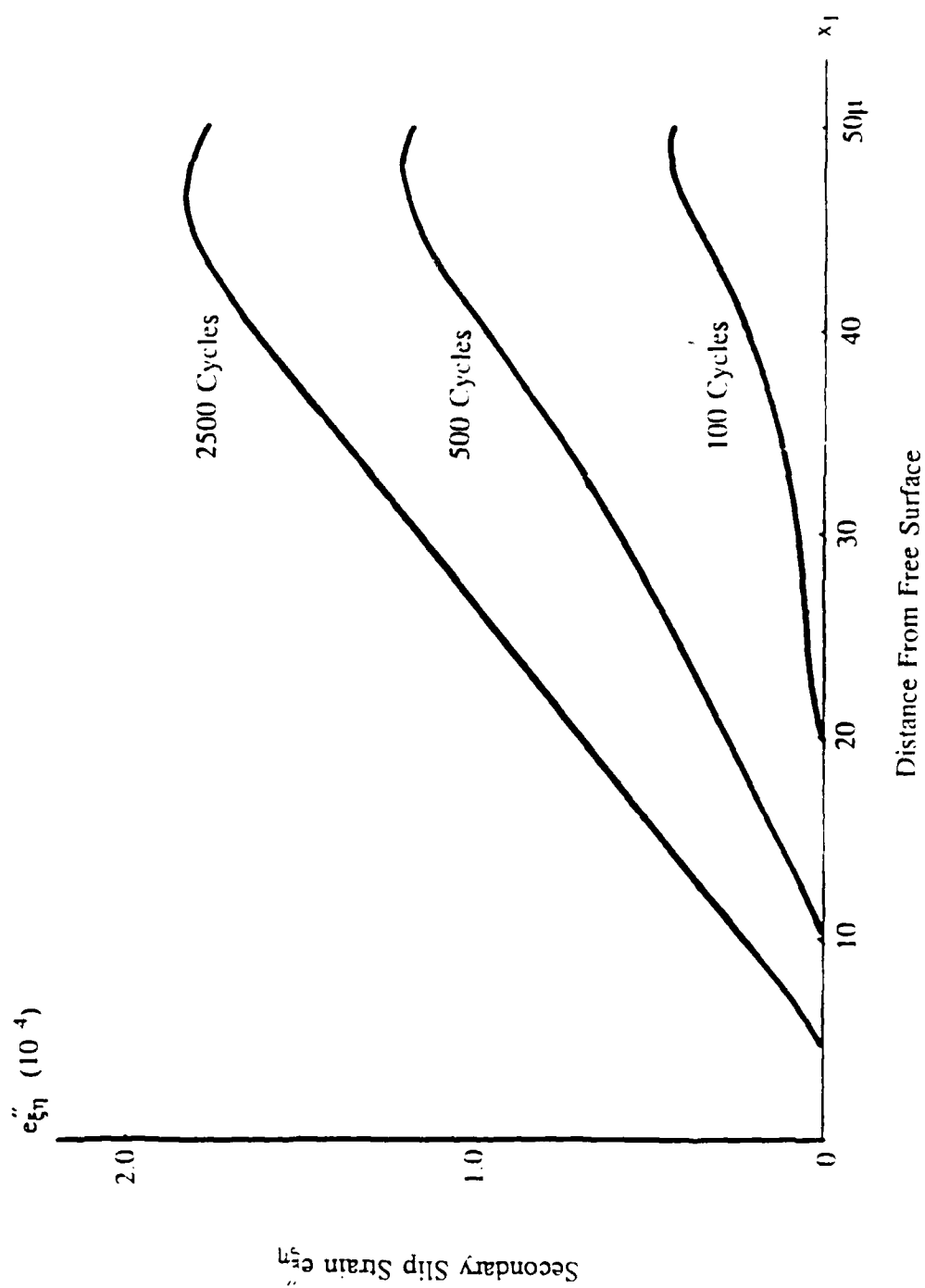
19

Fig. 3  Plastic Strain Distribution of the Secondary Slip System
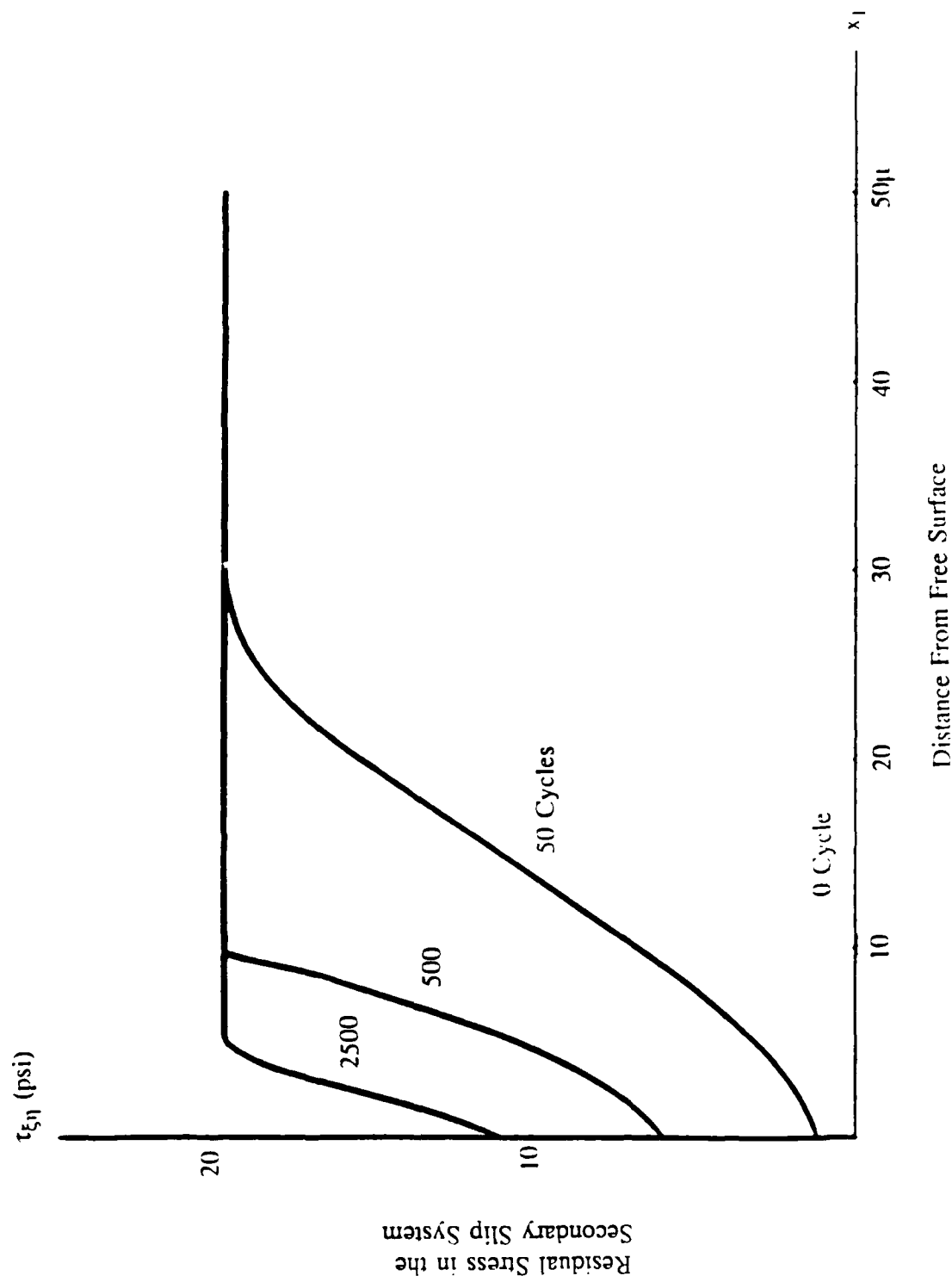
Fig.4  Residual Stress Distribution in the Secondary
Slip System

cycles of loading are shown in Fig. 7. It is seen for the case without considering the secondary slip, extrusion growth ceases as the extrusion approaches the static extrusion The plastic strains $e''_{\alpha\beta}$ in P and Q at the free surface, which represent the amount of extrusion or intrusion, with the secondary slip is four times that without the secondary slip.

## Conclusions

Under cyclic tension and compression the plastic shear strain growth $e''_{\alpha\beta}$ in P and Q were calculated with and without considering the secondary slip system $\xi\eta$. *The plastic strain $e''_{\xi\eta}$ in the secondary slip system has a component $e''_{\alpha\alpha}$ which has the same effect in causing $\tau^i_{\alpha\beta}$ in P and Q as $e^i_{\alpha\alpha}$. Hence $e''_{\alpha\beta}$ in P and Q with the secondary slip in the present case is four times more than that without the secondary slip.* Consequently, the extent of extrusion or intrusion in the cases with the secondary slip is greatly more than those without. This explains the observed extrusion growth beyond the static extrusion as reported by Mughrabi (1983) and explains that a face-centered polycrystal has greater extrusion height and intrusion depth than hexagonal polycrystals. The stress intensity factor of crack depends on the extent of extrusion and/or intrusion. Hence this extent is important for the study of crack initiation. The initial strain distribution $e^i_{\alpha\alpha}$ assumed in the slice R is arbitrary. Similar calculations can be made for other initial strain distributions. The present method of analysis satisfies the equilibrium, continuity of displacement and slip characteristics of the crystals.
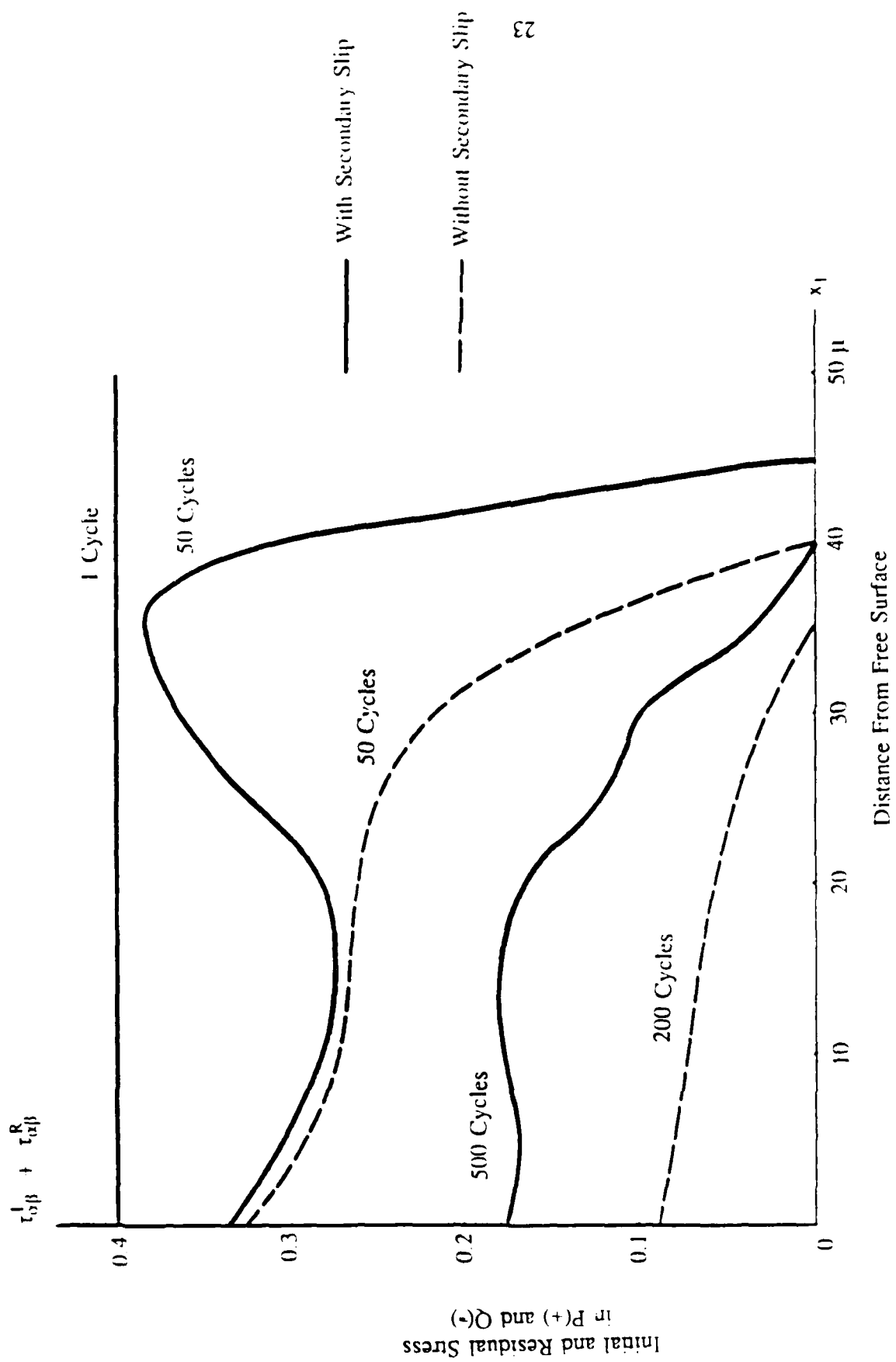
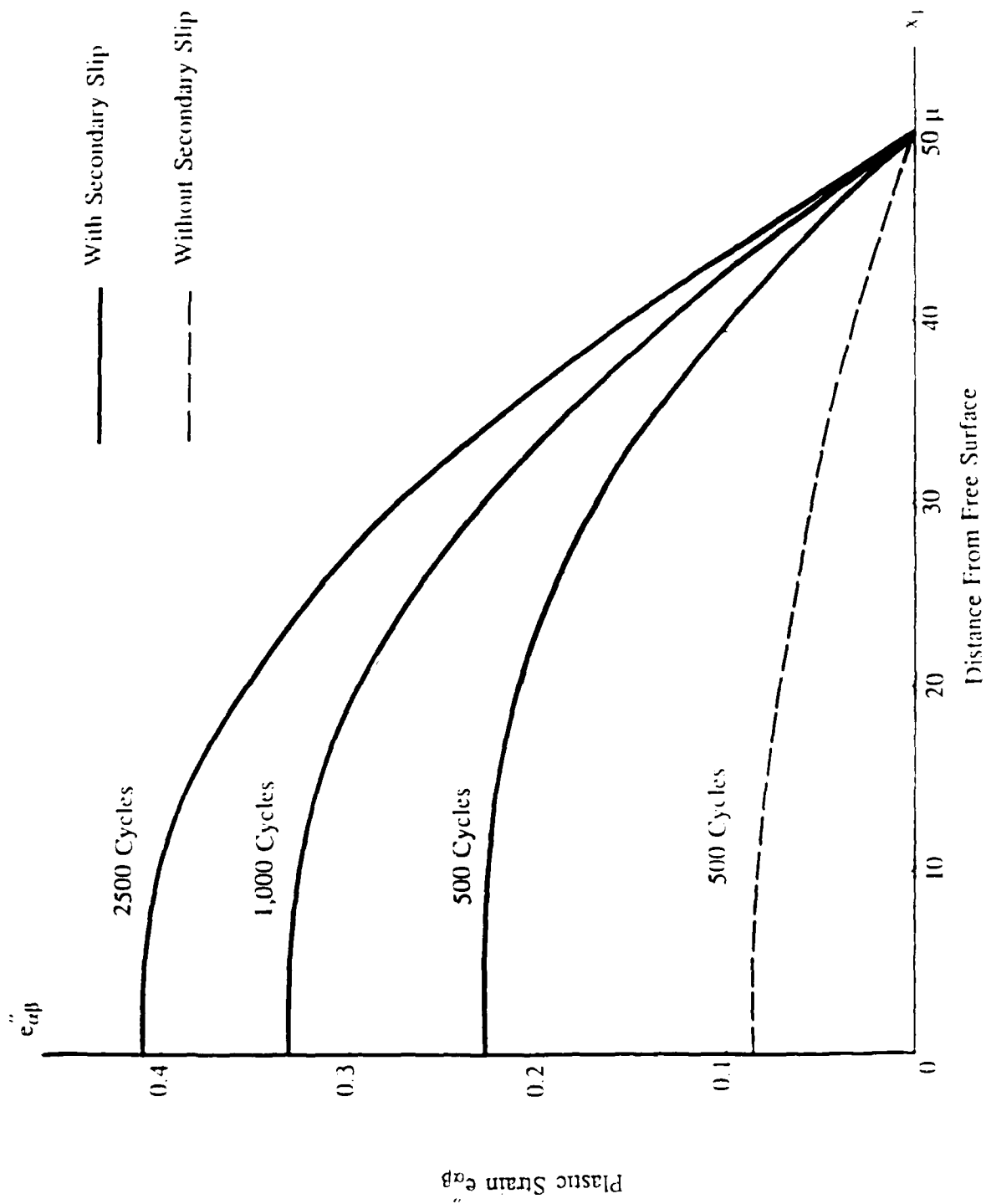Fig. 5  Initial and Residual Stress Distribution
in P and Q (P and Q opposite sign)
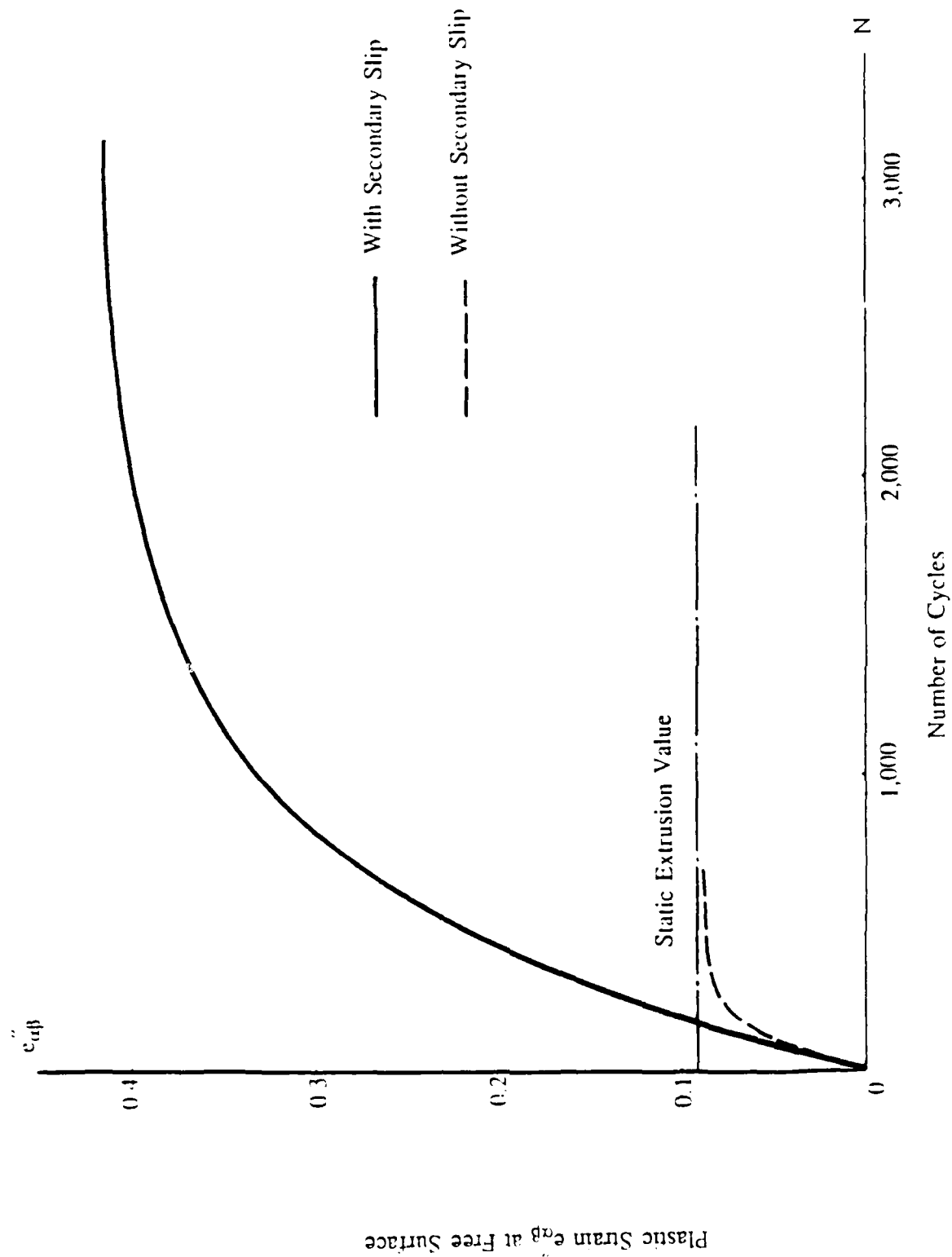
23

Fig. 6  Plastic Strain Distribution

Fig. 7  Plastic Strain Buildup at the Free Surface

## Acknowledgments

# References

1.  Antonopoulus, J.G., Brown, L.M., and Winter, A.J., 1976, Phil. Mag. 34, 549-563.

2.  Brown, A.F., 1952, Adv. Phys. 1, 427.

3.  Brown, L.M. and Ogin, S.L. 1984, "Fundamentals of Deformation and Fracture," Eshelby Memorial Symposium 500-528.

4.  Buckley, S.N. and Entwistle, K.M., 1956, ACTA Metall. 4, 352-361.

5.  Charsely, P. and Thompson N, 1963, Phil. Mag. 8, 77-85.

6.  Cottrell, A.H. and Hull, D. 1957, Proc. Rog. Soc. A. 202-211.

7.  Eshelby, J.D. 1957. Proc. Roy. Sec. A 241 pp. 376-396.

8.  Essmann, V., Gosele V. and Mughrabi H. 1981, Phil, Mag, 44. 405-426.

9.  Finney, J.M. and Laird C. 1975, Phil. Mag. 31, 339-366.

10. Forsyth, P.J.E. 1953 Nature 171, 172.

11. Forsyth, P.J.E. 1954, J. Inst. Metals 82, 449-454.

12. Grosskreutz, J.C. 1971 Phys. Stat. Solids (b) 47, 359-396.

13. Hull, D. 1958, J. Inst, Metals, 86, 425.

14. Kennedy, A.J. 1963 "Process of Creep and Fatigue of Metals", John Wiley & Sons, pp. 331-346.

15. Laird, E. C. and Duquette D.J. 1972 "Corrosion Fatigue" Edited by Devereux O.F., McEviley, A.J. and Stachle, R.W. pp. 88-117

16. Lin, T.H. and Ito, Y.M. 1967 J. Appl. Phys. 3, 775-780.

17. Lin. T.H. 1968 "Theory of Inelastic Structures" John Wiley & Sons., pp. 48-49.

18. Lin, T.H. and Ito, Y.M. 1969 J. Mech. Phys. Solids 17, 511-527.

19. Lin, S.R. 1972 Ph.D. Thesis, Univ. Calif. Los Angeles.

20. Lin, S.R. and Lin, T.H. 1974 J. Mech. Phys. Solids, 22, 177-192.

21. Lin, T.H. 1977 Rev. Deformation Behavior Materials, Fdited by P. Felthom, Freund Publishing House, Israel, 264-314.

22.    Lin, T.H. and Lin, S.R. 1983. J. Appl. Mech. 50, 367-372.

23.    McEviley J. Jr. and Machlin E.S. 1959 Proc. Int. Conf. Atomic Mechanism of Fraction Technology, John Wiley & Sons.

24.    Meke, K. and Blochwitz, C. 1980 Phys. Stat. Sol. a 61, 5.

25.    Mott, N.F. 1958 ACTA Metall, 6, 195.

26.    Mughrabi, H. 1980 Microscopic Mechanisms of Fatigue Strength of Metals and Alloys. Vol. 3 Perganon Press.

27.    Mughrabi H., Wang R., Differt K. and Essmann V. 1983, Fatigue Mechanism, ASTM STP 811, p. 5-45.

28.    Parker, E.R., 1961 "Mechanical Behavior of Materials at Elevated Temperatures" Edited by Dorn J.E., McGraw-Hill Book Co. pp. 129-148.

29.    Snowden, K.V., 1963, ACTA Metallugica Vol. 11 No.7, 675-684.

30.    Thompson, N. Wadsworth N.J. and Louat N. 1956, Phil. Mag. 1, 113.

31.    Thompson, N. 1959 Proc. Int. Conf. Atomic Mechanism of Fraction Technology, John Wiley & Sons.

32.    Winter, A.T. 1974, Phil. Mag. 30, 719-738.

33.    Wood, W.A. 1956 "Fatigue in Aircraft Structures", Edited by A.F. Freudenthal. Academic Press, New York. pp. 1-19.

34.    Wood, W.A. and Bendler, A.M. 1962, Trans. Metall. Soc. AIME 224 180-186.

35.    Wood, P.J. 1973, Phil. Mag. 30, 719-738.